Nano Research 2017, 10(6): 1880–1887
DOI 10.1007/s12274-016-1370-9
Research Article
ISSN 1998-0124
CN 11-5974/O4

Graphene-carbon nanotube hybrid films for high-performance flexible photodetectors

Yujie Liu, Yuanda Liu, Shuchao Qin, Yongbing Xu, Rong Zhang, and Fengqiu Wang (✉)

School of Electronic Science and Engineering and Collaborative Innovation Center of Advanced Microstructures, Nanjing University, Nanjing 210093, China

Received: 21 August 2016
Revised: 11 November 2016
Accepted: 15 November 2016

KEYWORDS
graphene,
carbon nanotube,
van der Waals heterostructures,
flexible photodetector

ABSTRACT

Graphene is being actively explored as a candidate material for flexible and stretchable devices. However, the development of graphene-based flexible photonic devices, i.e. photodetectors, is hindered by the low absorbance of the single layer of carbon atoms. Recently, van der Waals bonded carbon nanotube and graphene hybrid films have demonstrated excellent photoresponsivity, and the use of vein-like carbon nanotube networks resulted in significantly higher mechanical strength. Here, we report for the first time, a flexible photodetector with a high photoresponsivity of ~ 51 A/W and a fast response time of ~ 40 ms over the visible range, revealing the unique potential of this emerging all-carbon hybrid films for flexible devices. In addition, the device exhibits good robustness against repetitive bending, suggesting its applicability in large-area matrix-array flexible photodetectors.

1 Introduction

One-dimensional carbon nanotubes (CNTs) and two-dimensional graphene, the two most extensively investigated carbon allotropes for photonic applications [1, 2], exhibit advantageous properties such as high carrier mobility, broadband optical absorption, and environmental robustness [3–6]. Owing to the compatibility with large-scale processing, CNT thin films (or networks) and chemical vapor deposition (CVD) grown graphene are the most preferred material forms for practical applications involving high-volume production [7–10]. Compared with individual CNTs, which exhibit room-temperature mobility as high as 79,000 $cm^2/(V{\cdot}s)$ [11], CNT networks typically exhibit lower mobility (~ 10–100 $cm^2/(V{\cdot}s)$) and operating speeds, due to the existence of inter-tube Schottky barriers, and other morphological factors [12–16]. On the other hand, the low optical absorption and the ultrafast photocarrier recombination in graphene severely limit its photoresponsivity [17, 18].

Recently, ultra-thin all-carbon nanostructures comprising single-walled carbon nanotubes (SWNTs) and graphene heterostructures bonded covalently [19–21] or by van der Waals forces [22–24] have been developed, and they display superior properties compared with

Address correspondence to fwang@nju.edu.cn

the individual constituent materials. Current efforts are focused on the synthesis of a graphene-SWNT hybrid system with tailored microscopic morphology. The successful syntheses of both "rebar graphene" [20] and "rivet graphene" [21] illustrates the feasibility of flexible tuning of the physical properties of the graphene-SWNT hybrid. Another equally important route is to explore device applications based on such all-carbon membranes [23, 24]. Graphene-based photodetectors have been widely investigated. Even though high-speed devices employing intrinsic graphene have been operated at several tens of GHz, the relatively low responsivity (~10^{-3} A/W) [17] remains a deterrent for practical applications. Photogating of graphene has been the most successful approach for achieving enhanced photoresponsivity; by employing a quantum dots layer, photoresponsivity up to 10^7 A/W has been demonstrated. However, it invariably leads to a compromised response time [25]. A high-performance photodetector with a balanced overall performance was recently achieved by preparing van der Waals heterostructures of graphene-SWNT on a SiO_2/Si substrate. The device exhibited a photoconductive gain of 10^5 together with a fast response time (~100 μs), thus illustrating the potential of the graphene-SWNT hybrid for light harvesting applications that require large sensing area, high photoresponsivity and high speed [23]. The interfacial charge transfer dynamics within such hybrid nanostructures is also resolved through a combination of Raman and photocurrent spectroscopy techniques [26].

Flexible devices with optoelectronic functionalities integrated on bendable plastic substrates have attracted significant attention for their wide applicability in paper displays, smart windows, and wearable devices [27–32]. In contrast to rigid devices, the designing of flexible devices requires intrinsically stiff and bendable substrates that are engineered to withstand high levels of strain [33]. Remarkably, graphene-SWNT assemblies exhibit extraordinary mechanical flexibility and stretchability as well as electrical and optical conductivity, making them promising candidates for flexible optoelectronics [24, 34, 35]. In this work, we demonstrate for the first time, a fully flexible photodetector utilizing a graphene-SWNT hybrid film as the light harvesting layer. The photodetector on the flexible platform exhibits a high photoresponsivity of ~51 A/W and a fast response speed of ~40 ms over the visible wavelength range. In addition, our devices are stable under severe bending conditions, and are free from pronounced degradation even after a large number of bending cycles.

2 Results and discussion

The fabrication process of the graphene-SWNT hybrid films on polyethylene terephthalate (PET) substrate is shown in Fig. 1(a). As an initial step, homogeneous SWNT solutions with appropriate densities were spin-coated onto the PET substrate, which formed sparse network-like SWNT thin films. Subsequently, CVD-grown monolayer graphene was transferred atop the SWNT networks. We used a suitable geometry to avoid the degradation of charge transfer at the graphene-nanotube interface caused by the residual polymethyl methacrylate (PMMA) used for the transfer of graphene [36]. The morphology of the fabricated hybrid films on the PET substrate was examined by scanning electron microscopy (SEM) and the images are shown in Fig. 1(b). The SWNTs were sparsely distributed on the PET substrate and covered by a large flake of graphene sheet. The Raman spectrum of the hybrid films on the PET substrate (Fig. 1(c)) also showed pronounced peaks of the graphene-SWNT heterostructures, which are similar to the signatures on the SiO_2/Si substrate reported previously [23, 26]. As can be seen from Fig. 1(d), the resulted hybrid thin films on the PET substrate exhibit high transparency over the entire visible range. Typically, the transmittance of the hybrid thin films on the PET substrate reaches up to ~83% at the wavelength of 532 nm, which is approximately 5% lower than that of the pure PET substrate. Enhanced absorption in the ultra-violet range was also observed, which is an inherent feature of carbon nanomaterials [23]. The inset of Fig. 1(d) presents a photograph that manifests the good transparency of the graphene-SWNT hybrid films on the PET substrate.

Figure 2(a) schematically illustrates the flexible photodetector based on the graphene-SWNT hybrid films fabricated on the PET substrate. Characteristics of the photoresponse of the flexible devices were

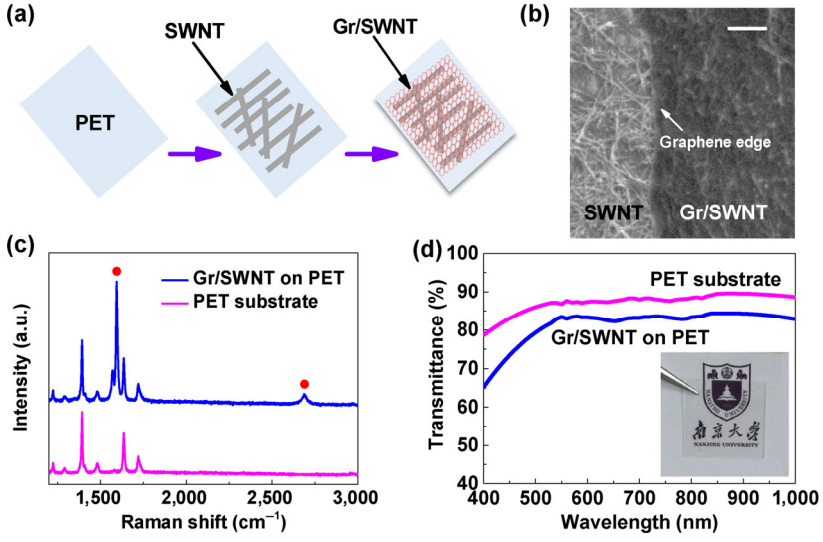

Figure 1 Characterization of the as-fabricated graphene-SWNT hybrid films on the PET substrate. (a) Schematic procedure for the preparation of the graphene-SWNT hybrid films on the PET substrate. (b) SEM image of the hybrid thin films on the PET substrate (scale bar: 1 μm). (c) Raman spectra obtained using 514 nm excitation laser. The red dots denote the pronounced peaks of the graphene-SWNT hybrid films. (d) Vis–NIR transmittance spectra of the graphene-SWNT hybrid films. The photograph in the inset shows the good visible transparency of the hybrid films on the PET substrate.

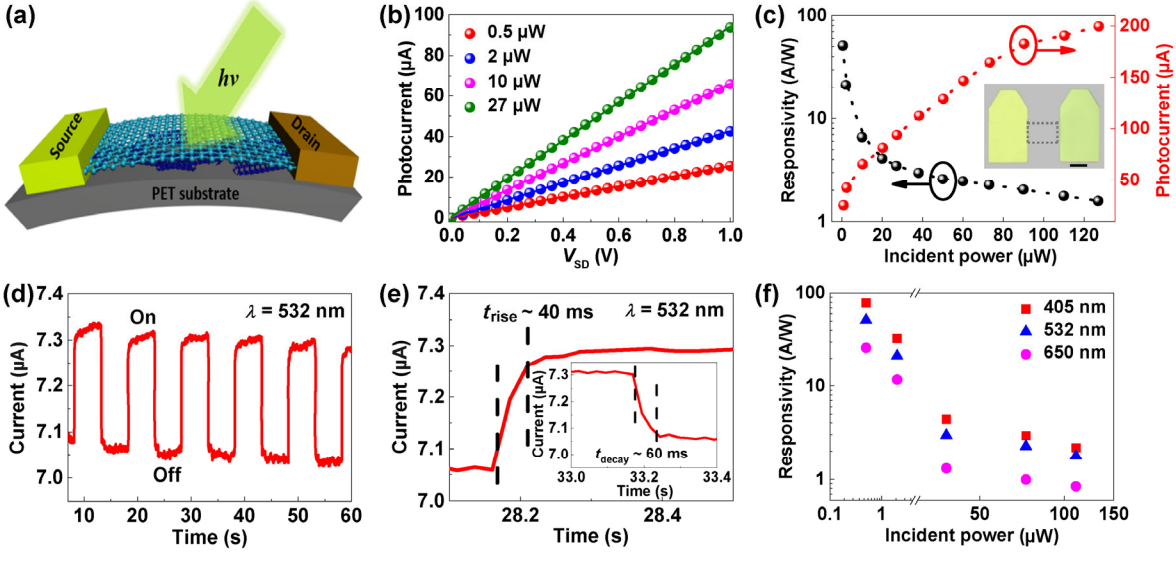

Figure 2 Characterization of the photoresponse of the flexible graphene-SWNT photodetectors. (a) Schematic illustration of the flexible photodetector based on the SWNT-graphene hybrid films fabricated on the PET substrate. (b) Dependence of the photocurrent on the source-drain voltage under the illumination of 532 nm laser. (c) Responsivity and photocurrent of the devices as functions of the incident light power at 532 nm and a source-drain voltage of 1 V. Inset: microphotograph of the fabricated device; the dashed square represents the graphene-SWNT channel (scale bar: 50 μm). (d) Time-dependent photoresponse of the flexible devices at 532 nm and a source-drain voltage of 0.01 V. (e) The enlarged rise and decay edges of a cycle. The rise time is defined as the time interval for the response to rise from 10% to 90% of its saturated value, so as the decay time. (f) Photoresponsivity as a function of the incident light power at wavelengths of 405, 532, and 650 nm, respectively.

measured using a laser diode operating at 532 nm under vacuum. Figure 2(b) shows the photocurrent as a function of the source-drain voltage (V_{SD}) under different illumination levels. It is clear that the photocurrent depends linearly on the V_{SD}. A high bias voltage increases the carrier drift velocity, and

reduces the carrier transfer time across the channel, giving rise to more effective separation and capture of the photogenerated carriers. The dependence of the photocurrent and the responsivity on the incident power is plotted in Fig. 2(c). As typically seen for graphene-based hybrid phototransistors [37], the photocurrent increases with increase in the incident power, while the corresponding photoresponsivity decreases due to the saturated absorption of illumination and the screening effect. It is worth noting that the responsivity of our detectors reaches ~51 A/W under a low illumination power of 0.5 μW at 532 nm, which is on a par with that of the gold oxide-graphene heterojunction device (58 A/W at 500 nm) [38]. The graphene-SWNT hybrid films generally exhibit faster speeds when compared with devices employing hybrids of graphene/transition metal dichalcogenides [39–43]. The drastically enhanced photoresponsivity is the result of the effective built-in electrical field at the graphene-SWNT junctions, which facilitates the separation of the photogenerated electron–hole pairs and reduces the charge carrier recombination at the interface [23]. The temporal response is measured by periodically turning the 532 nm light on and off at a bias voltage of 0.01 V, as presented in Fig. 2(d). The current level was invariant after several light irradiation cycles, indicating the good reversibility and the reliability of the devices. From Fig. 2(e), the response time was estimated to be ~40 ms, which is faster compared with the previously reported flexible graphene photodetectors (on the order of seconds) [44–46]. Such a prominent increase in the speed is attributed to the fast transfer of the carriers between the two carbon allotropes with intimate electronic coupling [23, 26]. Characteristics of the photoresponse of the devices in the ambient condition were also investigated. The results are very similar to those obtained in vacuum, except for a slightly lower dark current. With further optimization, the performance of the devices based on the all-carbon films may approach that of the InP nanowire-based devices which exhibit the best responsivity and temporal characteristics [47].

Furthermore, the broadband photoresponsivity was investigated in the visible range (by using diodes at 405, 532, and 650 nm) and the results are shown in Fig. 2(f). Higher responsivities were always observed at low values of the incident power, and the photoresponsivity was higher at shorter wavelengths. Such a spectral response is compatible with the absorption of the graphene-SWNT hybrid, which is fundamentally determined by the saddle-point exciton resonance in the ultra-violet region [23]. As with all the graphene-based photodetectors, our devices are expected to operate in the UV range, with enhanced performance.

Flexible optoelectronics are subject to a variety of mechanical deformations, thus, the mechanical flexibility and the durability under a bending stress are important figure-of-merits concerning practical applications. In order to assess the bending stability of the flexible graphene-SWNT hybrid photodetectors, the flexible devices were arranged on a cylindrical apparatus with three different radii of curvatures (k, k = 0.3, 0.6, and 0.9 cm^{-1}), and the photoresponse was measured while the devices were bent, as shown in Fig. 3(a). The I–V curves showed no discernible changes under the three different bending curvatures (Fig. 3(b)), which indicates the good adhesion to the substrate and the stable Ohmic contact between the electrodes and the graphene-SWNT channel under harsh bending conditions. It is to be noted that a good Ohmic contact is crucial for the unobstructed injection of the carriers at the junction between the channel and the electrodes [48]. Figure 3(c) displays the photocurrent dependence of the flexible devices under different bending curvatures. The photocurrent is almost invariant when compared with the original value. Significantly, the temporal photoresponse did not show degradation even under the maximum curvature of bending (k = 0.9 cm^{-1}) as illustrated in Fig. 3(d). These results indicate that the heterogeneous integration of the SWNTs and the graphene film on the thin pliable substrate has the potential for real-world applications in the areas of portable or wearable optoelectronics.

Durability is another equally crucial aspect concerning the practical applicability of the flexible devices. The fatigue cycling performance of our devices was evaluated as shown schematically in the inset of Fig. 4(a). The flexible devices were bent consecutively with a bending radius of 1.6 cm and their photoresponse was investigated under the illumination of 532 nm laser. The devices exhibited no delamination or cracks after the repeated bending tests, as confirmed

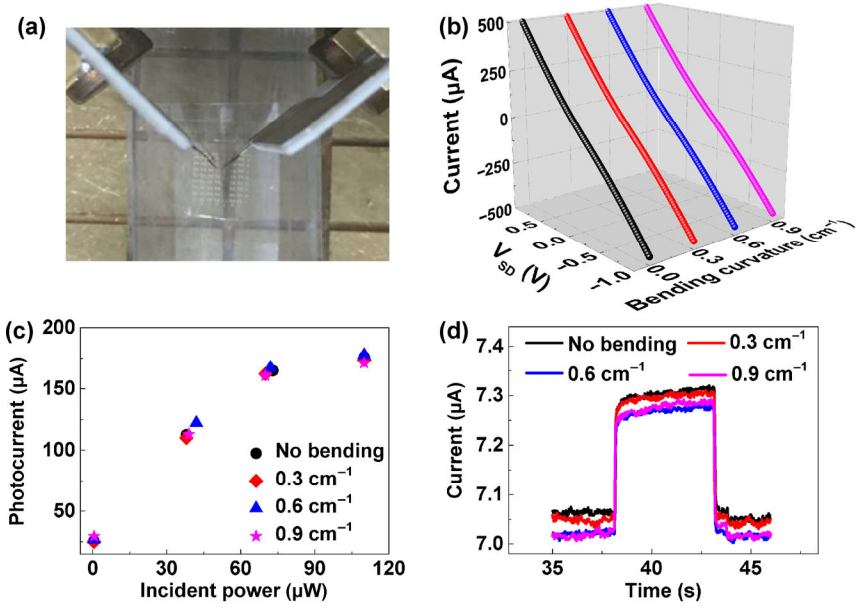

Figure 3 Photoresponse of the flexible graphene-SWNT photodetectors under different values of flexural strain. (a) Optical image of the set-up for the bending test of the flexible photodetectors. (b) *I*–*V* curves of the flexible devices under three different bending curvatures (k, k = 0.3, 0.6, and 0.9 cm^{-1}). (c) Characteristics of the photocurrent under different bending conditions at 532 nm. (d) Time-dependent photoresponse as a function of different bending curvatures under the illumination of 532 nm laser.

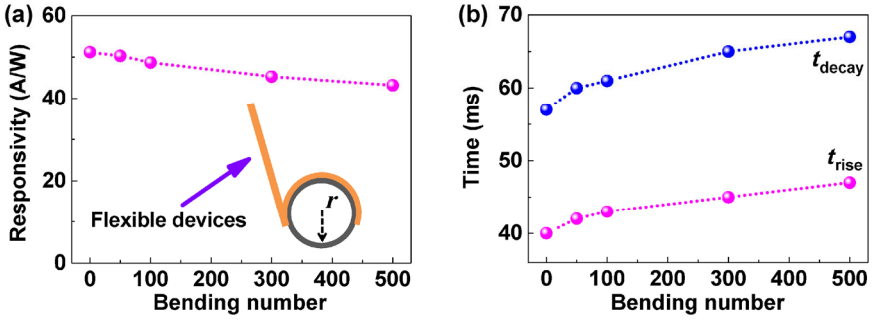

Figure 4 Performance of the flexible graphene-SWNT photodetectors under cyclic fatigue tests. (a) Responsivity as a function of the number of bending cycles at the radius (r) of 1.6 cm under the illumination of 532 nm laser. The inset shows the schematic diagram of the bending process. The flexible devices are attached to a glass vial on one end and pressed by a force on the other end. (b) Response time as a function of the bending cycle at 532 nm.

by the optical and the SEM images. Compared with the initial state, the parameters of the flexible devices were only slightly degraded even when the devices were subjected to 500 bending cycles, as shown in Figs. 4(a) and 4(b). These results demonstrate that the assembled flexible devices are not susceptible to strain and are electromechanically robust against repetitive bending.

3 Conclusions

In summary, a large-area, transparent and flexible photodetectors based on graphene-SWNT hybrid films on a PET substrate was demonstrated for the first time. These devices exhibited high photoresponsivity (~51 A/W) and fast response time (~40 ms) upon visible irradiation and are expected to operate well in the UV range. The fabricated devices show superior flexibility, good folding strength under harsh strain and bending states. It demonstrates that the all-carbon hybrid film is a highly robust material for practical applications in large-scale photosensors, flexible solar cells, etc. Furthermore, such a hybrid architecture will be fully compatible with graphene-based flexible electronic

components, facilitating the integration of large-scale optoelectronic functionality.

4 Methods

4.1 Fabrication of graphene-SWNT hybrid films and photodetectors

SWNT powders (purity: >90%, Carbon Solutions Inc.) were dispersed in N-methyl-2-pyrrolidone with a concentration of 0.1 mg/mL by ultrasonication for 3 h, followed by centrifugation at 10,000 g for 1 h. The CVD-grown monolayer graphene coating with PMMA on copper was immersed in ammonium persulfate for 3 h and deionized water for 30 min, respectively. Subsequently, the graphene film supported by the PMMA was transferred onto the SWNT/PET substrate. The PMMA was immediately removed using hot acetone (60 °C). The devices were fabricated using standard photolithography, metal deposition by electron beam evaporation, and lift-off. The electrodes were asymmetric; the source was Pd/Au (10 nm/40 nm) and the drain was Ti/Au (10 nm/40 nm). The graphene-SWNT channel was patterned using another photolithography technique and oxygen plasma etching.

4.2 Characterization and measurement of photoresponse

The Raman spectroscopy measurements were carried out on a Horiba Jobin Yvon LabRAM HR-800 Raman spectrometer with a 514 nm argon ion laser operated at 1 mW. The morphology of the coating was studied using SEM (JSM-7000F). The transmittance measurements were performed with a conventional tungsten halogen lamp (SLS202, Thorlabs) as the light source, and a monochromator (iHR 320, Horiba) was used in the wavelength selection mode. The photoresponse measurements were performed in a closed cycle cryogenic probe station under vacuum (<10^{-5} Torr) at room-temperature and the data were collected using a semiconductor parameter analyzer (Keithley 4200).

Acknowledgements

This work was supported in part by the National Basic Research Program of China (No. 2014CB921101); the National Natural Science Foundation of China (Nos. 61378025, 61427812, 61274102, and 61504056); Jiangsu Province Shuangchuang Team Program. Y. D. L. acknowledges funding of International Postdoctoral Exchange Fellowship Program (No. 20150023), the China Postdoctoral Science Foundation (No. 2014M551558) and Jiangsu Planned Projects for Postdoctoral Research Funds (No. 1402028B).

References

[1] Avouris, P.; Freitag, M.; Perebeinos, V. Carbon-nanotube photonics and optoelectronics. *Nat. Photonics* **2008**, *2*, 341–350.

[2] Bonaccorso, F.; Sun, Z.; Hasan, T.; Ferrari, A. C. Graphene photonics and optoelectronics. *Nat. Photonics* **2010**, *4*, 611–622.

[3] Meunier, V.; Souza Filho, A. G.; Barros, E. B.; Dresselhaus, M. S. Physical properties of low-dimensional sp^2-based carbon nanostructures. *Rev. Mod. Phys.* **2016**, *88*, 025005.

[4] Itkis, M. E.; Niyogi, S.; Meng, M. E.; Hamon, M. A.; Hu, H.; Haddon, R. C. Spectroscopic study of the Fermi level electronic structure of single-walled carbon nanotubes. *Nano Lett.* **2002**, *2*, 155–159.

[5] Falvo, M. R.; Clary, G. J.; Taylor, R. M., 2nd.; Chi, V.; Brooks, F. P., Jr.; Washburn, S.; Superfine, R. Bending and buckling of carbon nanotubes under large strain. *Nature* **1997**, *389*, 582–584.

[6] Lee, C.; Wei, X. D.; Kysar, J. W.; Hone, J. Measurement of the elastic properties and intrinsic strength of monolayer graphene. *Science* **2008**, *321*, 385–388.

[7] Wu, Z. C.; Chen, Z. H.; Du, X.; Logan, J. M.; Sippel, J.; Nikolou, M.; Kamaras, K.; Reynolds, J. R.; Tanner, D. B.; Hebard, A. F. et al. Transparent, conductive carbon nanotube films. *Science* **2004**, *305*, 1273–1276.

[8] Zhang, X. B.; Yu, Z. B.; Wang, C.; Zarrouk, D.; Seo, J. W. T.; Cheng, J. C.; Buchan, A. D.; Takei, K.; Zhao, Y.; Ager, J. W. et al. Photoactuators and motors based on carbon nanotubes with selective chirality distributions. *Nat. Commun.* **2014**, *5*, 2983.

[9] Li, X. S.; Cai, W. W.; An, J.; Kim, S.; Nah, J.; Yang, D. X.; Piner, R.; Velamakanni, A.; Jung, I.; Tutuc, E. et al. Large-area synthesis of high-quality and uniform graphene films on copper foils. *Science* **2009**, *324*, 1312–1314.

[10] van der Zande, A. M.; Barton, R. A.; Alden, J. S.; Ruiz-Vargas, C. S.; Whitney, W. S.; Pham, P. H. Q.; Park, J.; Parpia, J. M.; Craighead, H. G.; McEuen, P. L. Large-scale arrays of single-layer graphene resonators. *Nano Lett.* **2010**, *10*, 4869–4873.

[11] Dürkop, T.; Getty, S. A.; Cobas, E.; Fuhrer, M. S. Extraordinary mobility in semiconducting carbon nanotubes. *Nano Lett.* **2004**, *4*, 35–39.

[12] Buldum, A.; Lu, J. P. Contact resistance between carbon nanotubes. *Phys. Rev. B* **2001**, *63*, 161403.

[13] Nirmalraj, P. N.; Lyons, P. E.; De, S.; Coleman, J. N.; Boland, J. J. Electrical connectivity in single-walled carbon nanotube networks. *Nano Lett.* **2009**, *9*, 3890–3895.

[14] Lyons, P. E.; De, S.; Blighe, F.; Nicolosi, V.; Pereira, L. F. C.; Ferreira, M. S.; Coleman, J. N. The relationship between network morphology and conductivity in nanotube films. *J. Appl. Phys.* **2008**, *104*, 044302.

[15] Snow, E. S.; Novak, J. P.; Campbell, P. M.; Park, D. Random networks of carbon nanotubes as an electronic material. *Appl. Phys. Lett.* **2003**, *82*, 2145–2147.

[16] Itkis, M. E.; Borondics, F.; Yu, A. P.; Haddon, R. C. Bolometric infrared photoresponse of suspended single-walled carbon nanotube films. *Science* **2006**, *312*, 413–416.

[17] Xia, F. N.; Mueller, T.; Lin, Y. M.; Valdes-Garcia, A.; Avouris, P. Ultrafast graphene photodetector. *Nat. Nanotechnol.* **2009**, *4*, 839–843.

[18] Koppens, F. H. L.; Mueller, T.; Avouris, P., Ferrari, A. C.; Vitiello, M. S.; Polini, M. Photodetectors based on graphene, other two-dimensional materials and hybrid systems. *Nat. Nanotechnol.* **2014**, *9*, 780–793.

[19] Lv, R. T.; Cruz-Silva, E.; Terrones, M. Building complex hybrid carbon architectures by covalent interconnections: Graphene-nanotube hybrids and more. *ACS Nano* **2014**, *8*, 4061–4069.

[20] Yan, Z.; Peng, Z. W.; Casillas, G.; Lin, J.; Xiang, C. S.; Zhou, H. Q.; Yang, Y.; Ruan, G. D.; Raji, A.-R. O.; Samuel, E. L. G. et al. Rebar graphene. *ACS Nano* **2014**, *8*, 5061–5068.

[21] Li, X. L.; Sha, J. W.; Lee, S. K.; Li, Y. L.; Ji, Y. S.; Zhao, Y. J.; Tour, J. M. Rivet graphene. *ACS Nano* **2016**, *10*, 7307–7313.

[22] Lin, X. Y.; Liu, P.; Wei, Y.; Li, Q. Q.; Wang, J. P.; Wu, Y.; Feng, C.; Zhang, L. N.; Fan, S. S.; Jiang, K. L. Development of an ultra-thin film comprised of a graphene membrane and carbon nanotube vein support. *Nat. Commun.* **2013**, *4*, 2920.

[23] Liu, Y. D.; Wang, F. Q.; Wang, X. M.; Wang, X. Z.; Flahaut, E.; Liu, X. L.; Li, Y.; Wang, X. R.; Xu, Y. B.; Shi, Y. et al. Planar carbon nanotube-graphene hybrid films for high-performance broadband photodetectors. *Nat. Commun.* **2015**, *6*, 8589.

[24] Shi, J. D.; Li, X. M.; Cheng, H. Y.; Liu, Z. J.; Zhao, L. Y.; Yang, T. T.; Dai, Z. H.; Cheng, Z. G.; Shi, E. Z.; Yang, L. et al. Graphene reinforced carbon nanotube networks for wearable strain sensors. *Adv. Funct. Mater.* **2016**, *26*, 2078–2084.

[25] Konstantatos, G.; Badioli, M.; Gaudreau, L.; Osmond, J.; Bernechea, M.; Garcia de Arquer, F. P.; Gatti, F.; Koppens, F. H. L. Hybrid graphene-quantum dot phototransistors with ultrahigh gain. *Nat. Nanotechnol.* **2012**, *7*, 363–368.

[26] Liu, Y. D.; Wang, F. Q.; Liu, Y. J.; Wang, X. Z.; Xu, Y. B.; Zhang, R. Charge transfer at carbon nanotube-graphene van der Waals heterojunctions. *Nanoscale* **2016**, *8*, 12883–12886.

[27] Huang, L.; Huang, Y.; Liang, J. J.; Wan, X. J.; Chen, Y. S. Graphene-based conducting inks for direct inkjet printing of flexible conductive patterns and their applications in electric circuits and chemical sensors. *Nano Res.* **2011**, *4*, 675–684.

[28] Akinwande, D.; Petrone, N.; Hone, J. Two-dimensional flexible nanoelectronics. *Nat. Commun.* **2014**, *5*, 5678.

[29] Wang, K.; Wu, H. P.; Meng, Y. N.; Zhang, Y. J.; Wei, Z. X. Integrated energy storage and electrochromic function in one flexible device: An energy storage smart window. *Energy Environ. Sci.* **2012**, *5*, 8384–8389.

[30] Yeh, M. H.; Lin, L.; Yang, P.-K.; Wang, Z. L. Motion-driven electrochromic reactions for self-powered smart window system. *ACS Nano* **2015**, *9*, 4757–4765.

[31] Kim, D.-H.; Lu, N. S.; Ma, R.; Kim, Y.-S.; Kim, R.-H.; Wang, S. D.; Wu, J.; Won, S. M.; Tao, H.; Islam, A. et al. Epidermal electronics. *Science* **2011**, *333*, 838–843.

[32] Liang, Y.; Wang, Z.; Huang, J.; Cheng, H. H.; Zhao, F.; Hu, Y.; Jiang, L.; Qu, L. T. Series of in-fiber graphene supercapacitors for flexible wearable devices. *J. Mater. Chem. A* **2015**, *3*, 2547–2551.

[33] Nathan, A.; Ahnood, A.; Cole, M. T.; Suzuki, Y.; Hiralal, P.; Bonaccorso, F.; Hasan, T.; Garcia-Gancedo, L.; Dyadyusha, A.; Haque, S. et al. Flexible electronics: The next ubiquitous platform. *Proc. IEEE* **2012**, *100*, 1486–1517.

[34] Kholmanov, I. N.; Magnuson, C. W.; Piner, R.; Kim, J. Y.; Aliev, A. E.; Tan, C.; Kim, T. Y.; Zakhidov, A. A.; Sbervegleri, G.; Baughman, R. H. et al. Optical, electrical, and electromechanical properties of hybrid graphene/carbon nanotube films. *Adv. Mater.* **2015**, *27*, 3053–3059.

[35] Xiao, L.; Ma, H.; Liu, J. K.; Zhao, W.; Jia, Y.; Zhao, Q.; Liu, K.; Wu, Y.; Wei, Y.; Fan, S. S. et al. Fast adaptive thermal camouflage based on flexible VO_2/graphene/CNT thin films. *Nano Lett.* **2015**, *15*, 8365–8370.

[36] Pirkle, A.; Chan, J.; Venugopal, A.; Hinojos, D.; Magnuson, C. W.; McDonnell, S.; Colombo, L.; Vogel, E. M.; Ruoff, R. S.; Wallace, R. M. The effect of chemical residues on the physical and electrical properties of chemical vapor deposited graphene transferred to SiO_2. *Appl. Phys. Lett.* **2011**, *99*, 122108.

[37] Sun, Z. H.; Chang, H. X. Graphene and graphene-like two-dimensional materials in photodetection: Mechanisms and methodology. *ACS Nano* **2014**, *8*, 4133–4156.

[38] Liu, Y. L.; Yu, C. C.; Lin, K. T.; Yang, T. C.; Wang, E. Y.; Chen, H. L.; Chen, L. C.; Chen, K. H. Transparent, broadband, flexible, and bifacial-operable photodetectors containing a large-area graphene-gold oxide heterojunction. *ACS Nano* **2015**, *9*, 5093–5103.

[39] Withers, F.; Yang, H.; Britnell, L.; Rooney, A. P.; Lewis, E.; Felten, A.; Woods, C. R.; Romaguera, V. S.; Georgiou, T.; Eckmann, A. et al. Heterostructures produced from nanosheet-based inks. *Nano Lett.* **2014**, *14*, 3987–3992.

[40] Finn, D. J.; Lotya, M.; Cunningham, G.; Smith, R. J.; McCloskey, D.; Donegan, J. F.; Coleman, J. N. Inkjet deposition of liquid-exfoliated graphene and MoS_2 nanosheets for printed device applications. *J. Mater. Chem. C* **2014**, *2*, 925–932.

[41] Amani, M.; Burke, R. A.; Proie, R. M.; Dubey, M. Flexible integrated circuits and multifunctional electronics based on single atomic layers of MoS_2 and graphene. *Nanotechnology* **2015**, *26*, 115202.

[42] De Fazio, D.; Goykhman, I.; Yoon, D.; Bruna, M.; Eiden, A.; Milana, S.; Sassi, U.; Barbone, M.; Dumcenco, D.; Marinov, K. et al. High responsivity, large-area graphene/MoS_2 flexible photodetectors. *ACS Nano* **2016**, *10*, 8252–8262.

[43] Britnell, L.; Ribeiro, R. M.; Eckmann, A.; Jalil, R.; Belle, B. D.; Mishchenko, A.; Kim, Y. J.; Gorbachev, R. V.; Georgiou, T.; Morozov, S. V. et al. Strong light-matter interactions in heterostructures of atomically thin films. *Science* **2013**, *340*, 1311–1314.

[44] Liu, N.; Tian, H.; Schwartz, G.; Tok, J. B. H.; Ren, T. L.; Bao, Z. N. Large-area, transparent, and flexible infrared photodetector fabricated using p–n junctions formed by N-doping chemical vapor deposition grown graphene. *Nano Lett.* **2014**, *14*, 3702–3708.

[45] Sun, Z. H.; Liu, Z. K.; Li, J. H.; Tai, G. A.; Lau, S. P.; Yan, F. Infrared photodetectors based on CVD-grown graphene and PbS quantum dots with ultrahigh responsivity. *Adv. Mater.* **2012**, *24*, 5878–5883.

[46] Son, D. I.; Yang, H. Y.; Kim, T. W.; Park, W. I. Transparent and flexible ultraviolet photodetectors based on colloidal ZnO quantum dot/graphene nanocomposites formed on poly(ethylene terephthalate) substrates. *Compos. Part B: Eng.* **2015**, *69*, 154–158.

[47] Chen, G.; Liang, B.; Liu, Z.; Yu, G.; Xie, X. M.; Luo, T.; Xie, Z.; Chen, D.; Zhu, M.-Q.; Shen, G. Z. High performance rigid and flexible visible-light photodetectors based on aligned X(In, Ga)P nanowire arrays. *J. Mater. Chem. C* **2014**, *2*, 1270–1277.

[48] Zhang, W. J.; Chiu, M. H.; Chen, C. H.; Chen, W.; Li, L. J.; Wee, A. T. S. Role of metal contacts in high-performance phototransistors based on WSe_2 monolayers. *ACS Nano* **2014**, *8*, 8653–8661.